Discrete Dynamics in Nature and Society, Vol. 4, pp. 99–124
Reprints available directly from the publisher
Photocopying permitted by license only

"Discrete" Oscillations and Multiple Attractors in Kick-excited Systems*

V. DAMGOV† and I. POPOV

Bulgarian Academy of Sciences, Space Research Institute, 6 Moskovska Str., 1000 Sofia, Bulgaria

(Received 6 March 1999)

A class of kick-excited self-adaptive dynamical systems is formed and proposed. The class is characterized by nonlinear (inhomogeneous) external periodic excitation (as regards to the coordinates of excited systems) and is remarkable for its objective regularities: the phenomenon of "discrete" ("quantized") oscillation excitation and strong self-adaptive stability. The main features of these systems are studied both numerically and analytically on the basis of a general model: a pendulum under inhomogeneous action of a periodic force which is referred to as a kicked pendulum. Multiple bifurcation diagram for the attractor set of the system under consideration is obtained and analyzed. The complex dynamics, evolution and the fractal boundaries of the multiple attractor basins in state space corresponding to energy and phase variables are obtained, traced and discussed. A two-dimensional discrete map is derived for this case. A general treatment of the class of kick-excited self-adaptive dynamical systems is made by putting it in correspondence to a general class of dissipative twist maps and showing that the latter is an immanent tool for general description of its behavior.

Keywords: Nonlinear dynamics, Pendulum, Twist maps, Bifurcations, Dynamical chaos

1. INTRODUCTION

The nonlinear theory of oscillations considers mainly the action of periodic forces which does not depend on the coordinates or are linear with respect to the coordinates of the excited systems (Minorsky, 1962; Migulin *et al.*, 1983; Chua, 1987; Butenin *et al.*, 1987; Hagedorn, 1988; Kapitaniak, 1991). Nonlinear-parametric phenomena in dynamical systems described by equations with polynomial nonlinearity have been studied as well (Gumowsky, 1989).

In this paper, we study the mechanism and features of the phenomenon of low frequency (LF) continuous oscillation excitation under the action of an external high frequency (HF) force, which

* An investigation supported by the National Science Fund of the Bulgarian Ministry of Education and Science under contract No. TH-549/95.

† Corresponding author. Bulgarian Academy of Sciences, Space Research Institute, JK "Mladost 1A", Bl. 522, Vh. 5, Ap. 98, 1784 Sofia, Bulgaria. Fax: (++359 2)981 3347. E-mail: vdamgov@bas.bg.

is nonlinear as regards the coordinates of the excited systems (Vaynshtein and Vakman, 1983; Damgov *et al.*, 1986; Landa and Douboshinsky, 1989; Damgov and Grinberg, 1991; Damgov and Douboshinsky, 1992). References as LF and HF are used only on a relative basis. In the common case, the phenomenon is manifested in all frequency bands in oscillation systems influenced by external HF periodic forces that are nonlinear with respect to excited system coordinates. The notion referred to as "nonlinear force with respect to the system coordinate" will be clarified below. Such a system can be regarded as a self-oscillating one with external HF power supply (Landa and Douboshinsky, 1989).

The investigation is motivated by a survey of the processes and phenomena based on inhomogeneous interaction, inertia particle properties, etc., known from mechanics, (SHF) electronics, techniques of particle acceleration, etc. (Bruk, 1990; Kanavetz *et al.*, 1991; Miroshin and Halidov, 1991; Sikri and Narchal, 1993). In each particular case and regime the interaction mechanisms has been revealed differently (for example, calling like self-modulation, grouping, phase selection and so on). However, all these mechanisms are based on a common principle: the external HF force exerts nonlinear impact with respect to the system motion coordinate.

The phenomenon of continuous oscillation excitation with an amplitude selected from a discrete set of possible stationary amplitudes will be demonstrated on the basis of a general model – a pendulum under inhomogeneous action of an external HF periodic force.

The pendulum is a well-known physical device intensively studied for over 300 years. At present, the pendulum is quite rightly considered to be one of the most general models in nonlinear dynamics (Strijak, 1981; Morozov, 1990; Liao, 1992; Mawhin, 1993; Heng *et al.*, 1994). In systems of "pendulum type", phenomena like resonance, frequency pulling, synchronization and stabilization, etc., have been discovered. In the early 50s N.N. Bogolyubov and P.L. Kapitza discovered a possibility to stabilize the upper unstable equilibrium point of pendulum by using weak HF modulation applied to the point of suspension – a phenomenon that is applied, for example, in heated plasma stabilization in experiments for thermonuclear reaction utilization (Strijak, 1981; Blackburn *et al.*, 1992; Yip and Dimaggio, 1993; Hastings and McLeod, 1993). It is not a mere coincidence that the quantum-mechanical radio-frequency-driven Josephson junction discovered recently as well as the charge-density wave transport process are completely analogous to the pendulum with its strong sinusoidal nonlinearity. The inexhaustibility of the pendulum as a general model is once again corroborated by the herewith presented phenomenon of continuous oscillation excitation with an amplitude belonging to a discrete set of possible stable amplitudes.

The phenomenon of J. Bethenod is well-known (Minorsky, 1962, p. 495). Essentially it consists of the following: if one provides a physical pendulum with a piece of soft iron and places the pendulum above a coil, the pendulum starts oscillating and reaches a stationary state with a constant amplitude. Several theories explaining this phenomenon were discarded before Y. Rocard formulated the differential equation describing a specific kind of parametric excitation (Minorsky, 1962).

Our main goal here is to discuss the case where an external periodical source acts on a part of the trajectory of a moving pendulum in the absence of a parametric influence. In actual fact, we shall discuss a class of systems with specific excitation – self-adaptive kick-excited systems. The kick-excitation can be represented by a short, as compared to the main oscillation period, action of an external periodic force.

Considered as a class of oscillating systems with special energy feeding, it is constructed on the base of nonlinear oscillators with one degree of freedom under external time-dependent force of special kind; hence, from mechanical point of view they are systems with one and a half degrees of freedom and three-dimensional phase space. Let us write the external force as a product of two terms – the first is

periodic function of the time t, and the second nonlinear function of the oscillator variable x:

$$\ddot{x} + 2\beta\dot{x} + f(x) = \varepsilon(x) \cdot \Pi(\nu t) \qquad (1)$$

In this equation, the form of function $\varepsilon(x)$, which in fact can be regarded as coordinate-dependent amplitude of the driving force, is essential. In general, it can be constructed in an arbitrarily complicated form. However, in this paper we shall deal only with a small but interesting class of such functions. Namely, we shall consider that $\varepsilon(x)$ is nonzero only in a narrow interval of x, much less than the typical amplitude of oscillation. Throughout this paper, the function $\varepsilon(x)$ will be referred to as *feeding function*, and the interval in which it is different from zero as an *active zone* of the system. Now it is clear where the appellation "kick-excited systems", or shortly "kick-systems", comes from. Here the external force acts as short impulses (kicks), much shorter than the period of oscillation, and during the rest of time the system moves freely. This separating of movement into a free, weak-dissipating part and short active part during which the external force imports energy in the system makes possible (and easy) theoretical treatment of the problem.

A typical example of feeding function which is suitable both to analytical calculations and numerical experiments is Π-shaped function around zero:

$$\varepsilon(x) = \begin{cases} F, & |x| \le d' \\ 0, & |x| > d' \end{cases} \quad d' \ll 1 \qquad (2)$$

For the most of this paper, our considerations of the kick-systems will be restricted only to this feeding function. Only at the end of the paper, a broader generalization of the kick-systems and their main features will be made, and then the general form of the systems will be examined.

The case discussed in the paper is rather self-affined and quantitatively similar to a well-known problem examined by Fermi. As an explanation for the origin of cosmic rays, Fermi proposed a mechanism of accelerating charged particles as a result of collisions with moving magnetic field structures. A great number of papers deal with the simplest model case – the so-called model of Fermi–Ulam (Holmes, 1982; Lichtenberg and Lieberman, 1982; Isomäki, 1990). In the setup of the Fermi–Ulam scattering problem a ball is made to fly and impact dissipatively between two walls: one fixed and the other sinusoidally vibrating. The amplitude of the wall vibration and the coefficient of restitution between the ball and walls control the ball dynamics.

In recent years, the possibility to use similar mechanism for boosting space rockets in the gravitational field of planets and stars has been discussed as a matter of principle in different sources. This is the model of so-called "gravitational engine" accelerating particles or bodies. The part of the vibrating plate may be played, for instance, by the field of a rotating binary star.

Similar phenomena occur in other subclasses of the class of kick-excited systems, e.g. in periodically kicked hard oscillators, ice–structure interaction models, kicked rotators, driven impact oscillators, cyclotron accelerators of charged particles or phenomena of grouping and phase selection of particles, some processes of interaction between electromagnetic waves and particle ensembles in the ionosphere and magnetosphere of the earth, phenomena of generating powerful LF waves in the near space given a cosmic electromagnetic background, "mega-quantum" resonance structure of the solar system, etc. (Isomäki *et al.*, 1985; Isomäki, 1990; Tung, 1992; Soliman and Thompson, 1992; Troesch *et al.*, 1992; Damgov and Douboshinsky, 1992; Cecchi *et al.*, 1993).

This paper deals with the common features in the behavior of pendulum with invariable parameters in new conditions, namely, the pendulum is affected by continuous periodical external constrained force which is inhomogeneous with respect to the coordinates of motion. We shall demonstrate the phenomenon of periodic motion with a discrete set of possible stable amplitudes as well as the conditions bringing about irregular motion of the pendulum.

Figure 1 presents a schematic diagram of the pendulum system under consideration. The deviation of the pendulum from the lower equilibrium

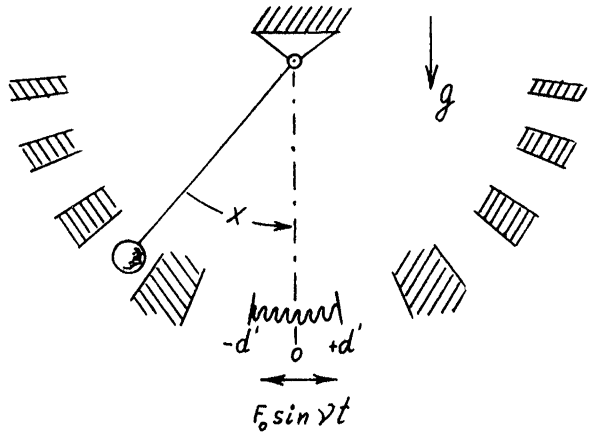

FIGURE 1 A schematic diagram of the kick-excited pendulum.

point is denoted by x. The external harmonic HF force $F = F_0 \sin \nu t$, where $F_0 = \text{const.}$, acts in a limited active zone $[-d', d']$ of the trajectory of the moving pendulum which is symmetrically positioned around the lower equilibrium point. This is the meaning of the notion "inhomogeneous action" related to the trajectory of pendulum motion, or the same can be expressed by the notion "nonlinear harmonic force" which should be understood as a nonlinear dependence of its amplitude on the coordinate of motion of the driven system – the pendulum. The direction of the external force action is parallel to the direction of the pendulum motion and it is periodically reversed. When, initially, the pendulum is driven out of equilibrium outside the zone $[-d', d']$ and released to oscillate, it periodically passes through the active zone and is subject to the action of the external force $F = F_0 \sin \nu t$. Under these conditions, a stationary mode of pendulum oscillation can be established with a quasiconstant amplitude, within one of the hatched areas of attraction in Fig. 1.

The particular stationary amplitude of pendulum motion is determined by the initial deviation and speed (i.e. by the initial conditions). Different modes of the pendulum motion are possible, and they depend on the initial conditions: the pendulum either catches up with one of the possible stationary orbits, or its motion is quickly damped. This is the heuristic value of the phenomenon – the presence of a possible discrete series of stationary amplitudes, i.e. a specific "quantization" of pendulum motion by intensity as a parameter. At the same time, there exist "forbidden" zones of initial conditions for which the motion is only a damped one. Obviously, there is a phenomenon of "quantized" oscillation excitation, a discretization of the dynamic states in a macro system. The excitation of one or the other amplitude depends on the initial conditions, provided that the other parameters and conditions are constant. We consider that the pendulum in this case is a self-oscillating system with a HF source or power supply (in contrast to the common perception that the self-oscillating systems should have a d.c. source of energy (Minorsky, 1962; Migulin *et al.*, 1983). In quantum mechanics, quantization (the notion of quanta) is postulated, and in the theory of relativity, quantization is not derived from geometric considerations. The discovered phenomenon shows that the "quantization" of energy transition into portions follows directly from mechanisms of the process and that it is defined from a formal mathematical point of view. The quasiharmonic oscillator obeys the classical laws to a greater extent than any other system. A number of problems related to quasiharmonic oscillators have the same solution in classical and quantum mechanics.

The layout of the current paper is as follows.

The results of the numerical investigations of the kick-systems are given in Section 2. In advance, we have to make a remark concerning our approach to the numerical experiment. It follows from the definitive Eqs. (1) and (2) that the evolution of studied systems is represented as a trajectory in three-dimensional phase space. The Poincaré map introduced in Section 2 for the kicked pendulum reduces the system variables down to two, corresponding to the oscillation energy and phase of the external force. The next step in our numerical analysis is to determine the stable stationary modes in the Poincaré map. It turns out that, at suitably chosen parameters, the system under study possesses a

family of stationary states. Besides them, periodic solutions with various low periods (3, 4, 5, ...) exist around fixed points (FPs) of the map at various parameter values. Such a variety of coexisting attractors makes us to determine their basins in the phase plane spanned by the energy–phase map variables. These basins are shown graphically like color images, where every pixel corresponds to an initial condition taken on a rectangular grid in the phase plane; the pixel color denotes the attractor the trajectory has been reached. These images allow us to make some qualitative conclusions about the system behavior. As an example, they clearly reveal the similarity of phase plane structure of the studied system (dissipative in its nature) with the hierarchy of resonances and Birkhoff islands, typical of vicinity of elliptic FPs in conservative two-dimensional maps. It also becomes clear that some areas in the phase plane exist in which close initial points evolve to completely different attractors; that way, the basin boundaries turn out to have fractal character.

The next step in numerical analysis is to study the evolution of the FPs and the most typical periodic points when one of the parameters, chosen by us as a control parameter, varies. In the class of systems studied in this paper, we have generally four parameters – damping β, amplitude F and frequency ν of the external force, and active zone width d'. We choose the forcing amplitude F as a control parameter; varying it, we obtain bifurcation curves of the stationary solutions, as well as those of the some typical periodic attractors. A special feature of the FPs is very interesting from practical point of view: when changing F within very large interval, the fixed value of the energy variable does not change noticeably and varies only in very narrow band (less than 1%).

The next Section 3 is devoted to theoretical examination of the kick-systems. It turns out that using some simplifying assumptions (neglecting the active zone width with respect to amplitude of the oscillations), we can obtain elementarily, in analytical form, the difference equation for the energy–phase variables of the Poincaré map. A very important result is that, in small amplitude approximation, the Poincaré map has the same form as well-known and widely studied dissipative standard map (DSM). Once given the form of difference equation, it is easy to reach some theoretical conclusions about the dynamics of kick-systems. For example, the linear stability analysis shows that the FPs are born for some value of parameter F via saddle-node bifurcation, and then, when increasing F, these solutions become unstable after period-doubling bifurcation. The theoretical parameter values for the bifurcation points obtained from our analysis turn out to be very close to the experimental ones given in Section 1. Moreover, following a work of Pakarinen and Nieminen (1983), an analytical study of periodic attractors surrounding FPs is carried out.

In Section 4, we briefly outline two other models that exhibit some typical features of the kick-system behavior. They are the Fermi–Ulam model about cosmic rays acceleration and the Zaslavskii map, describing evolution of a dynamical system (pendulum) under external forcing in the form of periodic in time δ-impulses. Even though these two models have been obtained for physical systems essentially different from the kick-systems described by Eq. (1), it turns out that there is a significant qualitative similarity in their dynamics and in the form of the model maps. The description of Ulam and Zaslavskii models in this paper is organized as a brief review: both systems have been subject to number of investigations by various authors, their behavior has been studied in detail and almost all features of their dynamics have been stressed. The review of these results, compared with our numerical results about the behavior of the kick-systems, provides us with additional arguments about the relation between the studied models. And finally, the class of dissipative twist maps appears as a general model, describing all the systems mentioned above. This class gives the link of the considered two-dimensional maps and Hamiltonian dynamics, especially those of the near-integrable systems (Lichtenberg and Lieberman, 1982).

The analytical form of the Poincaré map, derived in Section 3 for a particular case of kick-system, is generalized in the final Section 5 by varying the form of the system, i.e. if the nonlinear oscillator force $f(x)$ or feeding function $\varepsilon(x)$ in Eqs. (1) and (2) changes. The goal of this step is not only to generalize the way of reducing the kick-problems down to discrete maps but to make an attempt to reformulate the idea of kick-excited systems from the viewpoint of dissipative twist maps.

2. NUMERICAL EXPERIMENTS WITH KICKED PENDULUM

In this section our attention will be concentrated on a particular case of kick-system, chosen from the class described by Eqs. (1) and (2). Assuming the nonlinear force in (1) $f(x)=\sin x$, we come to a system which will be referred to as a *kicked pendulum*:

$$\ddot{x}+2\beta\dot{x}+\sin x=\varepsilon(x)F\sin(\nu t);\qquad \varepsilon(x)=\begin{cases}1, & |x|\le d'\\ 0, & |x|>d'\end{cases} \tag{3}$$

This particular model equation will serve as an example of a kick-system, which will be further examined both numerically (in this section) and analytically (in the next section).

In order to examine this system it is convenient to introduce the two-dimensional Poincaré surface in the following way. Because of the form of the external force in (3), phase trajectories *enter* the active zone through the two half-planes $\rho_{\pm}(x)=\pm d'$ (see Fig. 2). The two variables of the map are velocity $v=\dot{x}$ and phase of the external force $\varphi=\nu t \pmod{2\pi}$ in the moment of nth intersection of $\rho_{\pm}(x)$. One can see that velocity variable is related to the oscillation energy because $E=T+U=v^2/2+(1-\cos d')$; hence, the Poincaré map $(v,\varphi)_{n+1}=P(v,\varphi)_n$ is proved to be chosen in energy–angle variables.

It is easily seen that the trajectory passes twice for a period through this surface of section: once for positive and once for negative velocity. In general, we have to consider only one of these two intersections as an iteration of the Poincaré map, and the map points will be separated by one period of oscillation. But system (3) is invariant under transformation $(x,\dot{x},\varphi)\to(-x,-\dot{x},\varphi+\pi)$. Hence, a map with iterations separated by a half-period of oscillation can be used; it will include intersection points with both positive and negative velocities. In order to obtain such a map we have to change the phase variable with π when the velocity variable is negative, and replace the velocity with its absolute value. The map variables become

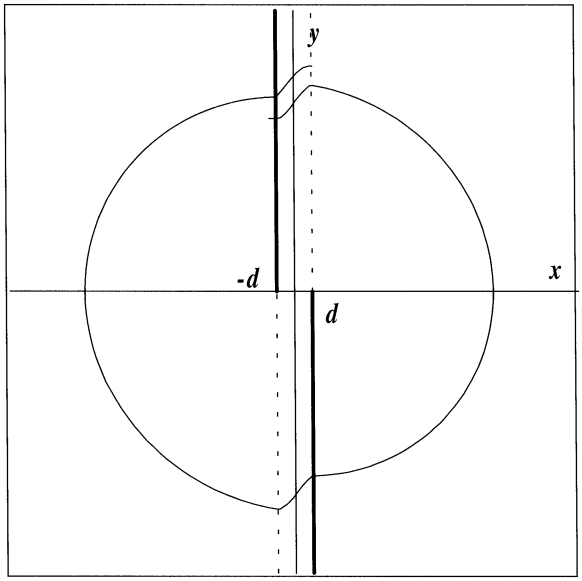

FIGURE 2 A typical trajectory of the kicked pendulum in the phase plane $(x,\dot{x})$.

$$v_n=|\dot{x}|;\ \varphi_n=\begin{cases}\nu t \pmod{2\pi}, & \dot{x}>0\\ \nu t+\pi \pmod{2\pi}, & \dot{x}<0\end{cases} \tag{4}$$

Equation (3) is numerically integrated using Runge–Kutta routine of fourth order. Taking into account that the right-hand side of (3) is discontinuous in $|x|=d'$ and the leaps in these points may reflect on the computational accuracy, a specific algorithm with variable time step is used. The

routine reduces automatically the time step in vicinity of leap points until sufficiently high accuracy is reached, and increases it at the regular parts of trajectory out of the active zone. Three of the system parameters are considered to be fixed: active zone half-width $d' = 0.025$, damping $\beta = 0.01$ and external force frequency $\nu = 51.0$. The external force amplitude plays the role of control parameter and only it is varied. When choosing values for the rest of parameters, as it will be shown in the next section, it is important to set small damping and high external frequency (much higher than the frequency of pendulum oscillations). The active zone is set to be sufficiently narrow; this requirement will be clarified below.

The stationary oscillations of the original system correspond, in the Poincaré map, to FPs. We have found that for some values of parameter F, $1 < F < 5$, the Poincaré map has multiple FPs, i.e. multiple periodic attractors for various parameters exist. For example, there are five stable FPs for $F = 1.5$, with velocities $v_i = \{0.2260; 0.7506; 1.0135; 1.1924; 1.3256\}$. In order to describe the system behavior when parameter F is varied, we present two different types of diagrams: color images of the basins of various attractors – FPs and most typical periodic points, and multiple bifurcation curves.

In order to obtain the attractor basins we set a 640×480 rectangular grid of initial conditions on the Poincaré surface and run each of them until the phase point converges to one of the attractors. A color image of the basins for $F = 1.5$ is presented in Fig. 3. The horizontal axis presents the velocity

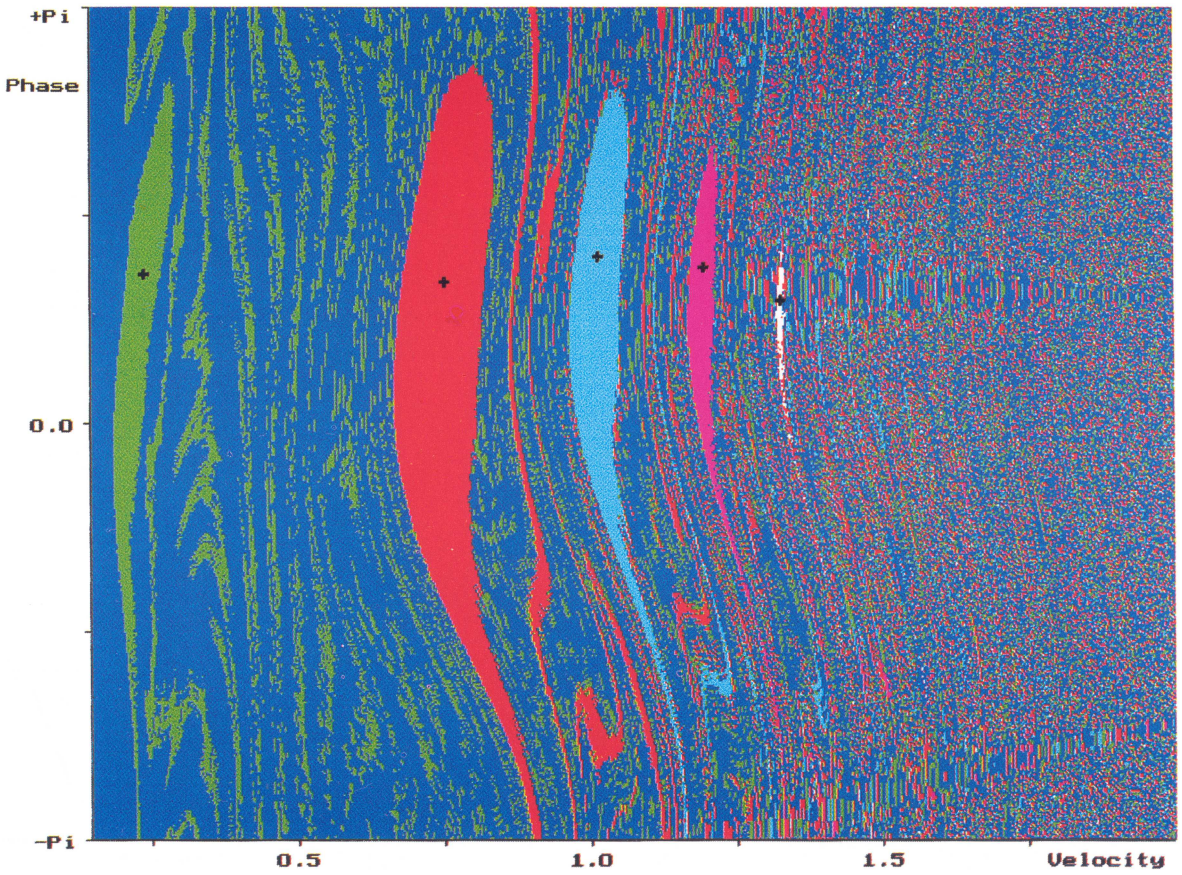

FIGURE 3 FPs and their basins of attraction of the kicked pendulum at $F = 1.5$. (See Color Plate I.)

in the interval $[0, 2]$; this interval assures that the pendulum motion remains finite, i.e. rotations around the hanging point are not considered. The phase variable is presented in the vertical axis. All the five FPs mentioned above and their basins are clearly seen in Fig. 3; the fixed points are marked by crosses, and each basin is denoted by different color. The basins have very complicated shape: they all have wide oval areas surrounding the FPs but there are also long and narrow "tails" getting out of them and completely disjoint set of points spread over the rest of state space. In this way, the complex, interwoven structure of the basins shows that they seem to have fractal boundaries (see, for example, McDonald *et al.*, 1985). Moreover, the extremely scattered areas far from the FPs lead to a very strong dependence of the final state of the system on the initial conditions: extremely small changes in the initial conditions make the system to jump from one basin to another.

Besides the five basins of the FPs, there is also an area colored in dark-blue in Fig. 3. It corresponds to initial conditions that converge to another stable orbit – a small limit cycle that falls entirely in the active zone, between the planes $\rho_{\pm}(x)$. Therefore, this small limit cycle cannot be presented on the Poincaré surface. However, we are not interested in such orbits, because if the trajectory does not leave the active zone, the dynamics of (3) simply degenerates to $\ddot{x} + 2\beta\dot{x} + \sin x = F\sin(\nu t)$, i.e. to the common case of pendulum with external fast-oscillating sine forcing. Because of this fact, we have not studied the latter mode in the current paper. We will only mention that this limit cycle can be observed by choosing some other Poincaré surface (for example, the plane $x = 0$); it corresponds to fast oscillations with small amplitude and frequency equal to the driving one.

Let us now study the evolution of the attractor basins when the parameter F varies. Two color maps for $F = 2.5$ and $F = 3.4$ are presented in Figs. 4 and 5, respectively. First, it is seen from Fig. 4 that the basins of the first FP and the small limit cycle in the active zone are completely interwoven. Second, a periodic solution with period 5 appeared around the second FP, and a similar 3-periodic solution around the fourth FP. Third, new FPs are born in the higher-velocity area of the image with $F = 2.5$ that have not existed at $F = 1.5$; however, their basins are relatively small. Another 2-periodic solution appeared between the first and second FP. When F is further increased up to 3.4 (Fig. 5), FPs corresponding to higher energies are destroyed, a 3-periodic solution appears around the third FP, and the basins of these orbits become smaller. A new stable orbit with period 2×4 appears around the "lonely" 2-periodic solution.

All the color maps clearly indicate that various low-period $(3, 4, 5, \ldots)$ periodic solutions exist around the "mother" FPs for various values of parameter F; they are very typical for the studied system. Moreover, it can be expected that more complex periodic orbits (with period $M \times N$) exist around these solutions, and so on. Such orbits actually exist, but both their basins and parameter ranges of their existence are too small so it is not possible to find more of them on the color images. This complex set of periodic points in the Poincaré map is similar to the hierarchy of resonance KAM-curves and Birkhoff N-chains surrounding elliptic points in conservative maps. (Note that although system (3) is dissipative, the chosen damping is quite small and since the Jacobian of (4) depends on β like $J = 1 - O(\beta)$, the map is very near to conservative.) However, the phase space structure of the conservative maps is not stable under small dissipative perturbations (Lieberman and Tsang, 1985; Tsang and Lieberman, 1986). Under dissipative perturbations, KAM-curves are destroyed, and the elliptic points of the Birkhoff N-islands become N-periodic sinks. Hence, the period-N attractors around the FPs correspond to Birkhoff N-chains; $M \times N$ and higher subharmonics correspond to $M \times N$ chains around the elliptic points of the N-chains, and so on. In order to show the relation between conservative and weakly-dissipative dynamics, the structure of the Poincaré map of conservative kick-pendulum ($\beta = 0$ in (3)) is presented for two different parameter values: $F = 1.5$ (Fig. 6) and $F = 2.5$ (Fig. 7). A rough comparsion

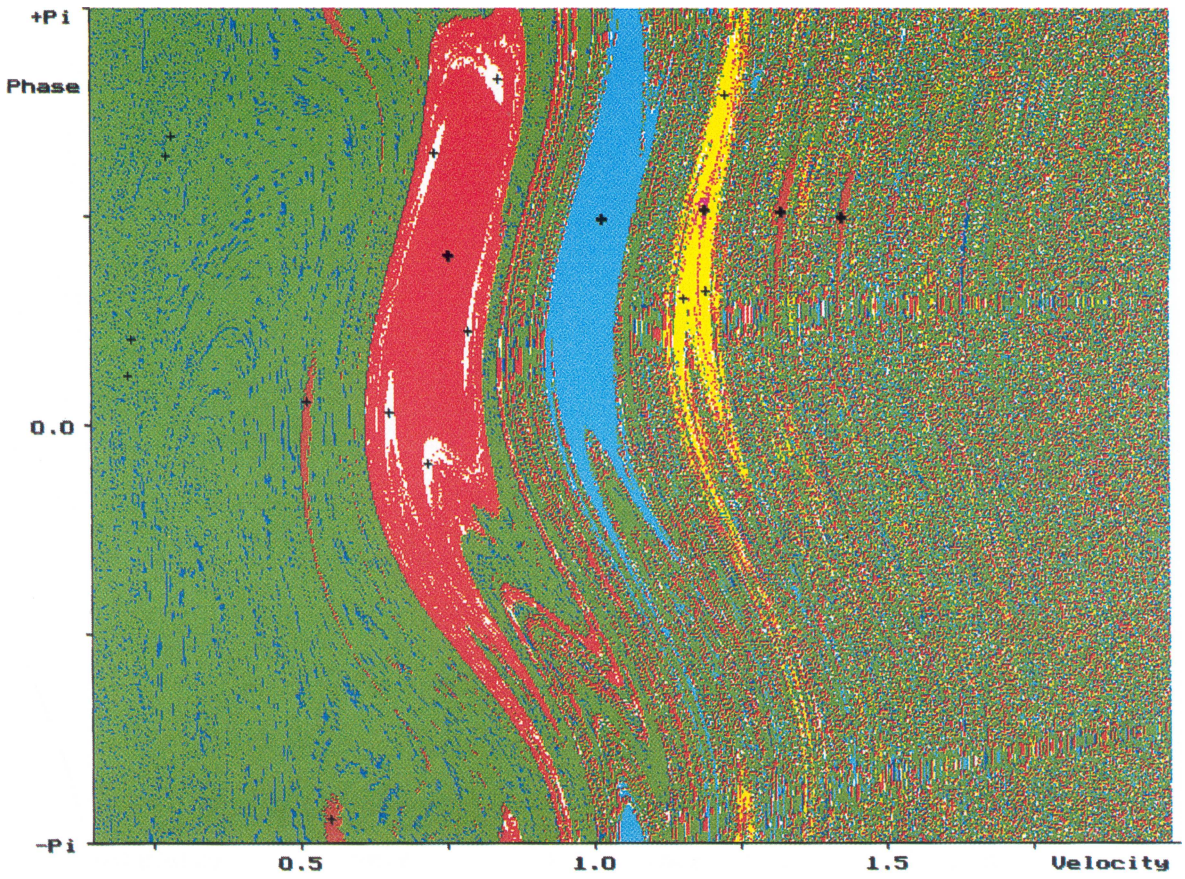

FIGURE 4 FPs, periodical points and their basins of attraction of the kicked pendulum at $F=2.5$. (See Color Plate II.)

with Figs. 3 and 4 immediately reveals the straight relationship between the periodic attractors and Birkhoff islands.

The bifurcation diagram shown in Fig. 8 shows the behavior of the whole family of FPs (black lines) and 3-periodic points (grey lines) when varying the parameter F; the vertical axis shows velocity variable. For clarity, the bifurcation curves of second and third FP are shown separately in Fig. 9 on a larger scale. It is evidently seen that the bifurcation behavior of the first FP (that with the lowest energy) is quite untypical with respect to the rest of them, corresponding to higher energies: it consists of several separated curves. A possible explanation is that the first orbit has too small amplitude and the phase point of the pendulum spends fairly long time in the active zone – several periods of the external force. For comparsion, the other FPs correspond to orbits which spend less than a period of external force in the active zone. Therefore, we can conclude that the requirement for narrow active zone is somewhat violated for the first orbit; it will be actually shown in the next section that the dynamics of kicked pendulum depends not exactly on the absolute half-width d but mostly on so-called *phase half-width* $\xi = \nu d'/\bar{v}$.

The FPs appear in the bifurcation diagram as a result of saddle-node bifurcations, and with increase of the parameter F they undergo period-doubling cascade. However, we must have in mind that the studied map (4) corresponds to a half-period but not a full period of motion. In that sense,

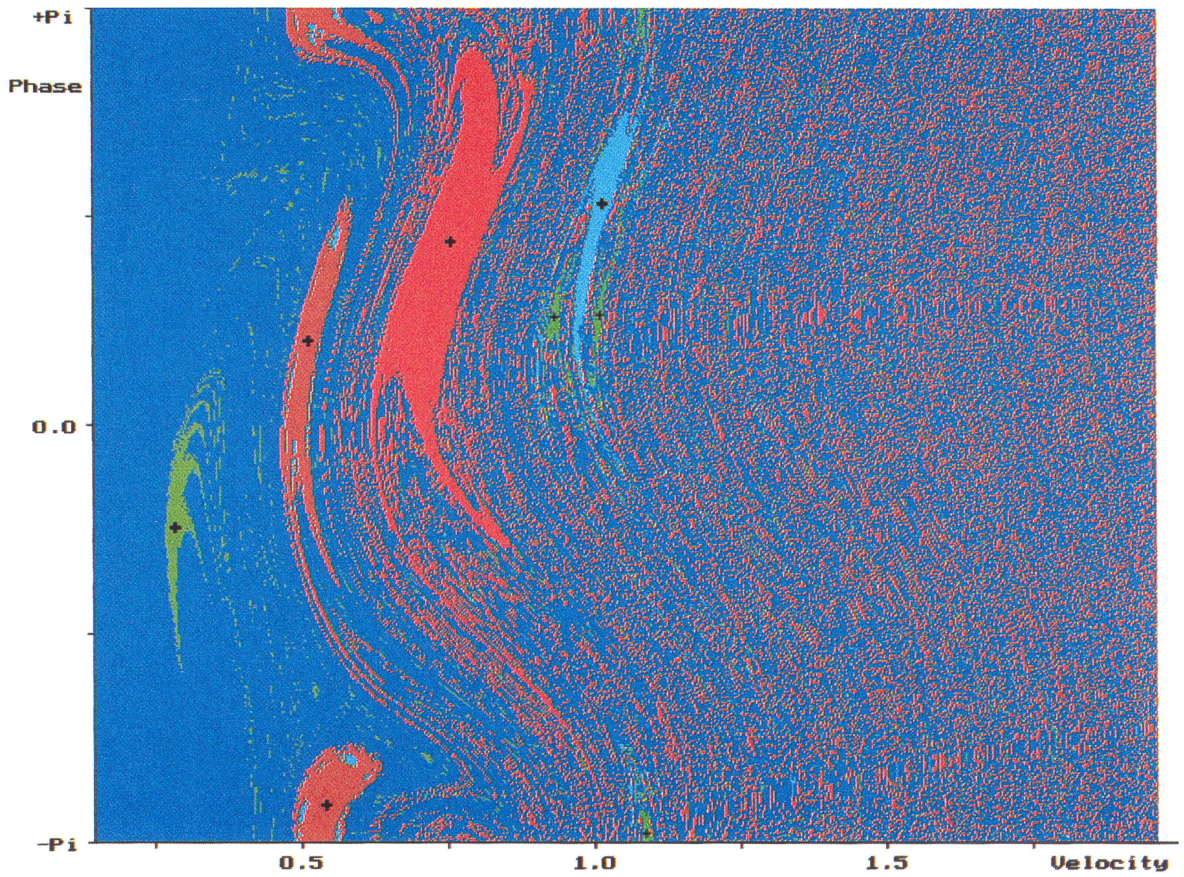

FIGURE 5 FPs, periodical points and their basins of attraction of the kicked pendulum at $F = 3.4$. (See Color Plate III.)

the first period doubling of a map FP corresponds to a symmetry-breaking bifurcation of an orbit in continuous phase space of initial system (3), and only the second period doubling of the FP becomes first period doubling of the orbit of (3). In other words, when constructing our Poincaré map, we have taken down the symmetry of the system because the half-period map does not already have the additional symmetry of initial system. This may be seen either from the bifurcation curve (there is not any symmetry-breaking before the first period doubling in Fig. 8), or from the stability analysis presented in the next section.

It is easily seen that the velocity variable of the FPs (hence the energy of oscillation) remains almost constant between the birth and period-doubling point, with variations less than 0.1%. Such a strong adaptivity of the system is due to the fact that the energy of the stable orbits, as it will be proven in the next section, is fully determined by the amplitude-dependence of the pendulum period but not by the external force F.

The mechanism of appearance of periodic points surrounding a given FP is similar to the appearance of Birkhoff N-islands around an elliptic point in conservative mappings. This mechanism is described in a paper of Pakarinen and Nieminen (1983). The main idea is that (in conservative case) a Birkhoff N-chain appears very near around an FP for some parameter value, and expands away when changing the parameter in the appropriate direction. Figure 9 shows that in the studied (dissipative) system, 3- and N-periodic attractors appear near the "mother" FP and run away from it with the

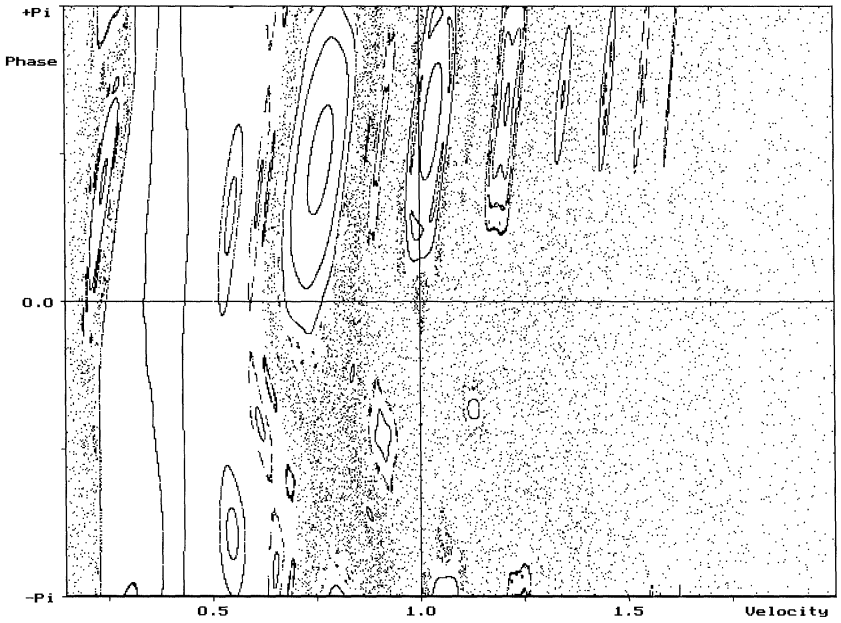

FIGURE 6 Structure of the Poincaré map of conservative kicked pendulum at $F = 1.5$.

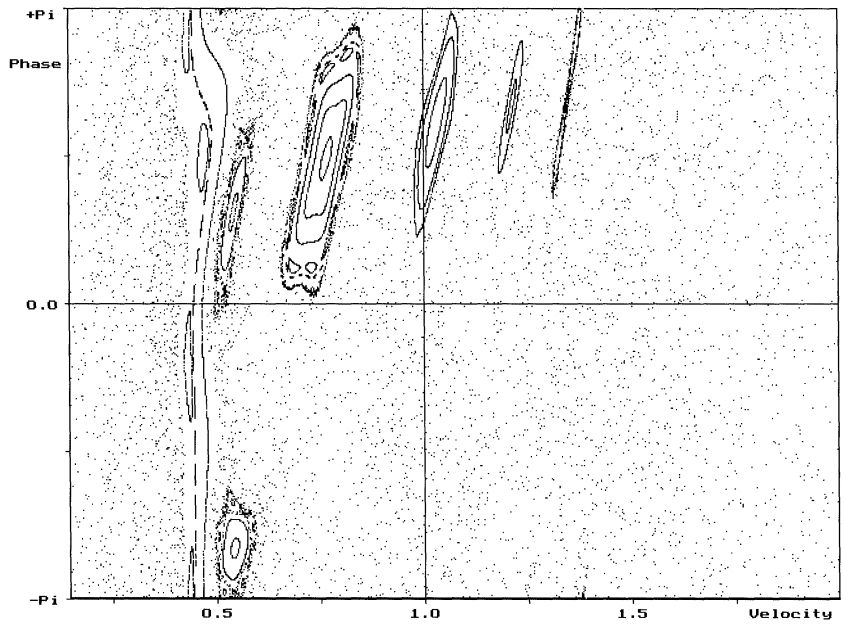

FIGURE 7 Structure of the Poincaré map of conservative kicked pendulum at $F = 2.5$.

increase of F. An interesting effect is that the 3-periodic attractor captures almost all attractor basins of the mother FP at the moment of birth, except for a very small area in the center and three tiny strips getting out of it (see Fig. 4). However, the mother FP remains stable: the 3-furcation (Pakarinen and Nieminen, 1983) which produces 3-periodic point does not involve it but most of

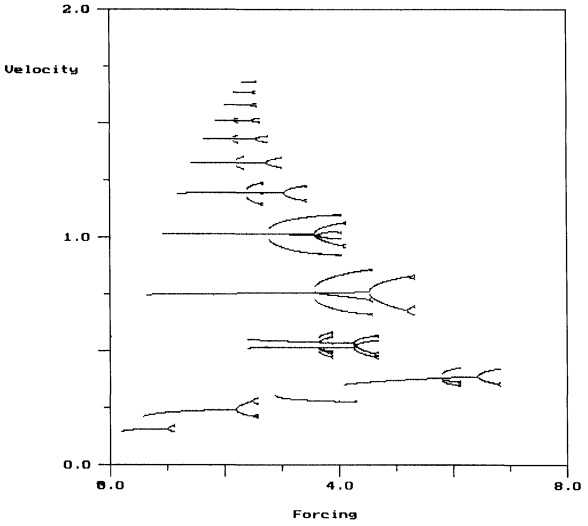

FIGURE 8 Bifurcation diagram for the whole family of FPs (black) and period-3 points surrounding each of them (grey).

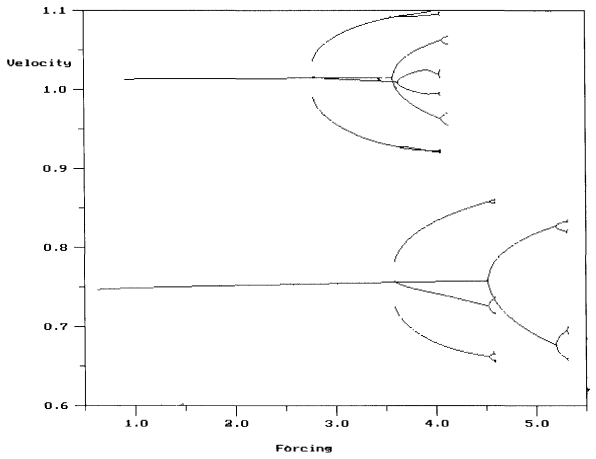

FIGURE 9 Bifurcation diagram for the second and third FP and the corresponding period-3 solutions

its basin is found to be transferred to the new-born periodic solution. Actually, the periodic points rapidly expand away from the mother FP when increasing F, their basins contract in size and finally the periodic points undergo a cascade of period-doubling bifurcations in the same manner as FPs.

All the period-doubling cascades in Fig. 8 lead in universal way to strange attractors (Schuster, 1984).

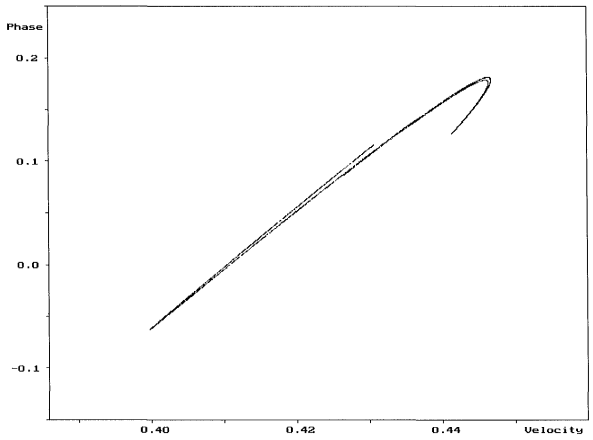

FIGURE 10 A strange attractor of the kicked pendulum for parameters $\beta = 0.2$ and $F = 11.9$.

However, these strange attractors are very small in size and exist for very narrow parameter range ($\sim 10^{-4}$); they are destroyed just after they are born. This phenomenon is due to the relatively small dissipation in the studied system. After reaching the Feigenbaum point F_∞, inverse period-doubling bifurcation sequence has to take place. nth inverse bifurcation produces strange attractor composed of 2^n isolated segments from one composed of 2^{n+1} segments; ideally, the cascade leads up to a single-segmented, chaotic strange attractor. However, in two-dimensional dissipative maps the inverse bifurcation sequence is truncated by boundary crisis which destroys the attractor (Schmidt and Wang, 1985; Chen *et al.*, 1986). Moreover, the point of boundary crisis comes very close to the Feigenbaum point when Jacobian of the map approaches unity (Chen *et al.*, 1986). In the studied low-damping case, these points are separated by an interval of order 10^{-4} at various attractors, and by reason of that it is practically impossible to find such thin strange attractor strips in Figs. 8 and 9. But if we choose relatively high damping, we can observe single-segmented strange attractors: one of them (found at parameters $\beta = 0.2$ and $F = 11.9$ is shown in Fig. 10.

After a particular attractor has been destroyed via boundary crisis, the trajectory corresponding

to it runs away from it and converges to one of the rest stable attractors. On the bifurcation diagram, it looks as if the system has suddenly jumped from one attractor to another. Here we must mention that there are two different types of boundary crises which truncate the inverse bifurcation sequence. If the destroyed attractor is the only one in the system, then its basin occupies the whole accessible phase plane; in some sense it has no boundaries and the crisis is not of boundary type but of interior type (Grebogi *et al.*, 1983).

Such a crisis is "chaos–chaos" compared with "chaos–order" that occurs in the studied map. In the latter case the dynamics after crisis is regular but in the former case the chaotic attractor suddenly changes its size and the character of motion (Grebogi *et al.*, 1983). However, all the crises in the kicked pendulum map are of boundary type due to the presence of multiple attractors. The only exception occurs when the last survived attractor undergoes crisis; in our map, such is the small limit cycle entirely closed in the active zone. For larger F (~ 10–30) very long transient motion is observed ($\sim 10^{-4}$ map iterations and even more) before the trajectory settles down on the small limit cycle. When increasing F, the transient time grows and the limit cycle expands in size; at about $F \approx 67$ it gets out of the active zone, becomes unstable and the system dynamics becomes totally stochastic.

3. THEORETICAL ANALYSIS OF THE KICKED PENDULUM

In this section, we present an approximate but simple derivation of two-dimensional map corresponding to the Poincaré map of kicked pendulum (3). The fact that Poincaré map (4) is defined in energy–phase variables prompts that we have to examine the energy balance of the system. The external force acts in such a way that the system receives energy only once in a half-period as a very short impulse; therefore, an expression for the incoming energy can be easily obtained. In order to simplify our calculations, we have to make two main assumptions concerning the system parameters. We assume weak positive dissipation ($0 < \beta \ll 1$) and thin active zone, i.e. phase trajectory crosses it for a time $t_{\text{zone}} \ll T$, where T is the half-period of oscillation. The two map variables will correspond to the total energy and the phase of the external force in the active zone center ($x = 0$).

The energy received for the one passing through active zone is

$$\Delta E_{\text{in}} = \int_{-d}^{d} F \sin(\nu t(x))\, \mathrm{d}x \tag{5}$$

Introducing phase variable $\psi = \nu t$ and assuming $\bar{v}$ is the average velocity in the active zone, one can obtain

$$\begin{aligned} \Delta E_{\text{in}} &= \int_{\psi_{\text{in}}}^{\psi_{\text{out}}} \frac{F}{\nu} \sin\psi \dot{x}\, \mathrm{d}\psi = \frac{Fv}{\nu} \int_{\psi_{\text{in}}}^{\psi_{\text{out}}} \sin\psi\, \mathrm{d}\psi \\ &= \frac{2Fv}{\nu} \sin\psi_0 \sin\xi = 2Fd' \frac{\sin\xi}{\xi} \sin\psi_0 \end{aligned} \tag{6}$$

Here we have introduced median phase $\psi_0 = (\psi_{\text{in}} + \psi_{\text{out}})/2$ and phase half-width of the active zone $\xi = (\psi_{\text{out}} - \psi_{\text{in}})/2 = \nu d'/\bar{v}$. Expression (6) can be further simplified by assuming small phase half-width $\sin\xi \cong \xi$; in this case, it becomes

$$\Delta E_{\text{in}} = 2Fd' \sin\psi_0 \tag{7}$$

Now we have to determine the energy loss of (3) for the time interval between two passings through the active zone, i.e. for a half of period. Under the assumption of thin active zone, it will be approximately equal to the energy loss in case of free damped pendulum, which is given by

$$\Delta E_{\text{out}} = 16\beta[E(m) - (1-m)K(m)] \tag{8}$$

Here $m = E_0/2$ and $E_0 = \dot{x}^2/2 + (1 - \cos x)$ is the full energy of the system, $K(m)$ and $E(m)$ are complete elliptic integrals of first and second kind, respectively. In case of small amplitudes (8) can be

simplified using the expansions

$$K(m) = \frac{\pi}{2}\left(1 + \frac{m}{4} + \frac{9}{64}m^2 + \cdots\right)$$
$$E(m) = \frac{\pi}{2}\left(1 - \frac{m}{4} - \frac{3}{64}m^2 + \cdots\right) \tag{9}$$

and keeping only terms of order up to m, one reaches

$$\Delta E_{\text{out}} = 4\beta K(m)E_0 = \beta T(m)E_0 \tag{10}$$

Here $T(m)$ is the period of pendulum oscillations, expressed as a function of its energy.

Let us now precisely define the map variables. The energy variable is $m = E_0/2$, and the phase one is the median phase defined in (6): $\theta = \psi_0$. In addition, we assume that m_n does not stand for the moment of nth passing the center of the active zone, but for the moment of $(n-1)$th leaving the zone; these moments are shown in Fig. 11. We used such a complicated notation because it simplifies

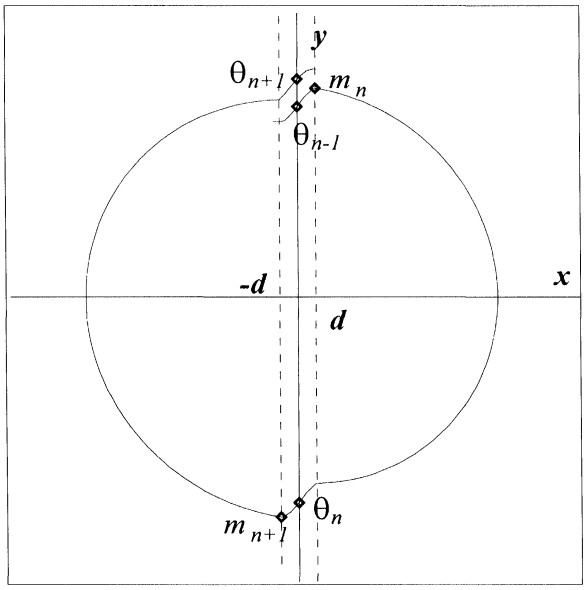

FIGURE 11 The phase points standing for consecutive iterations of the map variables along the trajectory.

the equation for evolution of phase variable. It becomes simply

$$\theta_{n+1} = \theta_n + \frac{\nu T}{2} + \pi$$
$$= \theta_n + 2\nu K(m_{n+1}) + \pi \pmod{2\pi} \tag{11}$$

The additional term $+\pi$ is introduced because of the symmetry of (3): it is invariant under transformation $(x, \dot{x}, \psi) \to (-x, -\dot{x}, \psi + \pi)$, and the subsequent passes through active zone occur for velocities with opposite signs (see Fig. 11). The balance of m is written as

$$m_{n+1} = m_n + \Delta\frac{E_{\text{in}}}{2} - \Delta\frac{E_{\text{out}}}{2}$$
$$= m_n + Fd' \sin\theta_n - \Delta\frac{E_{\text{out}}}{2} \tag{12}$$

Here we can use either the exact expression for the energy dissipation (8) or the small amplitudes approximation (10). In the first case, joining the equations for energy and phase variables, we obtain the two-dimensional map

$$m_{n+1} = m_n - 8\beta[E(m_n) - (1 - m_n)K(m_n)]$$
$$+ Fd' \sin\theta_n \tag{13}$$
$$\theta_{n+1} = \theta_n + 2\nu K(m_{n+1}) + \pi \pmod{2\pi}$$

In the case of small amplitudes approximation, expressing $K(m)$ only with terms of order up to m and assuming m and β are both small, the following approximate map is obtained:

$$m_{n+1} = m_n(1 - 2\pi\beta) + Fd' \sin\theta_n$$
$$\theta_{n+1} = \theta_n + (\nu + 1)\pi + \frac{\nu\pi}{4}m_{n+1} \pmod{2\pi} \tag{14}$$

Now one can easily see that this map is a particular case of so-called *dissipative standard map* (DSM) extensively studied in the literature (Bohr *et al.*, 1984; Schmidt and Wang, 1985; Casdagli, 1988):

$$r_{n+1} = br_n - \frac{k}{2\pi}\sin(2\pi\theta_n)$$
$$\theta_{n+1} = \theta_n + \omega + r_{n+1} \pmod{1} \tag{15}$$

Actually, one can reach up to DSM from (14) substituting $(m, \theta) \to (r = \nu m/8,\ \theta = \theta/2\pi)$ and introducing new parameters $b = J = 1 - 2\pi\beta$, $\omega = (\nu + 1)/2$ and $k = -16\pi F d'/\nu$.

This is a very important result. It links the studied kicked pendulum to another class of problems and, more precisely, to the problem of nonlinear rotator under external force acting as periodical in time δ-impulses. This problem is described by so-called *Zaslavskii map* which is closely related to DSM. On the other hand, DSM is very extensively studied in all aspects by many authors; a brief report about its more important features will be presented in the next section.

Let us now find the FPs (m^0, θ^0) of the map (13). The equation for m yields

$$Fd' \sin\theta^0 = 8\beta[E(m^0) - (1 - m^0)K(m^0)] \qquad (16)$$

and from equation for θ it follows that

$$2\nu K(m^0) = (2l - 1)\pi \qquad (17)$$

The last result shows that for a fixed value of the frequency ν the system possesses discrete set of stationary states m_l^0 for various values of l; the condition $K(m) \geq \pi/2$ requires $(2l - 1) \geq \nu$. Moreover, Eq. (17) completely determines the stationary values of the energy, hence the amplitude of oscillation. Taking into account only the first two terms in the expansion of $K(m)$ according to (9), one can find approximately

$$m_l^0 = 4\left[\frac{2l - 1}{\nu} - 1\right] \qquad (18)$$

That is the reason for which we call (17) a *discretization condition* for the system. Actually, the presence of a discrete set of FPs immediately follows from the fact that one of the map variables is phase one and is taken by modulo of 2π. This automatically yields the possibility of discrete set of solutions, each of them corresponding to increase of the phase variable with integer number of periods per iteration.

A very important consequence from the particular form of (17) is that the stationary energy does not depend on external force amplitude F, but only on its frequency; the same is valid for the amplitude of oscillations. That is the reason for the superstability of the kicked pendulum amplitude that has been observed in numerical experiments.

The same discretization condition can also be obtained using the assumption that in a stationary state the half-period of oscillation must be equal to *odd* number times the half-period of the external force. In case of thin active zone this yields

$$\frac{T}{2} = 2K(m_l^0) = (2l - 1)\frac{\pi}{\nu} \qquad (19)$$

which is exactly the same as (17). It is remarkable that the latter expression resembles a bit the condition for synchronization of a system: the period of oscillation becomes multiple of the external force period. But in contrast to the "normal" synchronization, in this case, the amplitude of the motion can get a discrete set of values for a particular choice of external frequency ν. Moreover, in the case of "normal" synchronization the amplitude varies continuously when the external force F is changed, but in the system studied here the discretization condition keeps it almost constant; only a very weak variation, due to the finite size of the active zone has been observed in numerical experiments (see the previous section). The energy balance of (13), respectively (3), holds due to the variation of the phase variable θ but not of the amplitude. Indeed, the expression for received energy (7) is proportional to sine of the middle phase ψ_0, so this variable can effectively control the energy balance.

The stationary value of the phase variable follows directly from (14):

$$\sin\theta_l^0 = \frac{8\beta[E(m_l^0) - (1 - m_l^0)K(m_l^0)]}{Fd'} \qquad (20)$$

and the restriction $|\sin\theta| \leq 1$ leads to

$$Fd' \geq F_{\text{sn}}d' = 8\beta[E(m_l^0) - (1 - m_l^0)K(m_l^0)] \qquad (21)$$

The latter result is a simple illustration of the fact that if either the amplitude F or the size of the active zone d' is too small, the system cannot receive enough energy in the active zone in order to compensate the dissipation for half-period. The value F_{sn} for which (21) turns into equality corresponds to saddle-node bifurcation point. In this point a pair of FPs is born, corresponding to two values of θ_l^0 satisfying (20) with respect to $\sin\theta_l^0$. It will be shown below that one of these two FPs is stable and the other is always unstable.

In order to examine the stability of the FPs (m_l^0, θ_l^0), we have to linearize (13) in its vicinity. This yields (in matrix form) the following system:

$$\begin{pmatrix} \delta m_{n+1} \\ \delta\theta_{n+1} \end{pmatrix} = \begin{pmatrix} 1-W & B \\ (1-W)C & 1+BC \end{pmatrix} \begin{pmatrix} \delta m_n \\ \delta\theta_n \end{pmatrix} = \hat{M} \begin{pmatrix} \delta m_n \\ \delta\theta_n \end{pmatrix} \tag{22}$$

where following notations are introduced:

$$W = 8\beta\left[\frac{\mathrm{d}E}{\mathrm{d}m} - (1-m_l^0)\frac{\mathrm{d}K}{\mathrm{d}m} + K(m_l^0)\right]; \quad B = Fd'\cos\theta_l^0; \quad C = 2\nu\frac{\mathrm{d}K}{\mathrm{d}m} \tag{23}$$

The linear stability condition is $|\lambda_{1,2}| < 1$, where $\lambda_{1,2}$ are the eigenvalues of the matrix $\hat{M}$ determined by $\det(\hat{M} - \lambda\hat{E}) = 0$. After some computations we obtain the stability interval

$$-(4-2W) < BC < 0 \tag{24}$$

or, after substitution from (23),

$$-4 + 16\beta\left[\frac{\mathrm{d}E}{\mathrm{d}m} - (1-m_l^0)\frac{\mathrm{d}K}{\mathrm{d}m} + K(m_l^0)\right] < 2\nu\frac{\mathrm{d}K}{\mathrm{d}m}Fd'\cos\theta_l^0 < 0 \tag{25}$$

It can be easily proved that the eigenvalues are strictly real at the ends of the interval. When $BC = 0$, $\lambda_1 = \pm 1$ and this corresponds to the saddle-node bifurcation; the condition for its occurrence expressed from (25) is $\cos\theta_l^0 = 0$, which is identical to the condition $|\sin\theta_l^0| = 1$ yielding expression (21) for saddle-node bifurcation value of parameter F.

When $BC = -(4-2W)$, $\lambda_2 = -1$ and this corresponds to period-doubling bifurcation. Writing the left inequality from (25) with respect to F, we can obtain the period-doubling value of the forcing. Assuming for simplicity the small amplitude case and expressing $K(m)$, $\mathrm{d}K(m)/\mathrm{d}m$ and $\mathrm{d}E(m)/\mathrm{d}m$ from expansions (9) up to terms of order m, we reach

$$Fd' < F_{\mathrm{pd}}d' = \sqrt{[2\pi\beta m_l^0(1+m_l^0/8)]^2 + \left[\frac{16}{\pi\nu(1+9m_l^0/8)}\right]^2} \tag{26}$$

In order to test our theoretical expression for F_{pd} against the bifurcation values of F numerically obtained in the previous section, we evaluate it for parameters $\nu = 51.0$, $\beta = 0.01$ and $d' = 0.025$ for the fourth stable orbit, which corresponds to $l = 29$ and $m_l^0 = 0.378$. We find the theoretical value $F_{\mathrm{pd}}^{\mathrm{the}} = 2.96$, compared to the experimental value $F_{\mathrm{pd}}^{\mathrm{exp}} = 3.04$ obtained in numerical simulations. So we can conclude that our analytical results are in relatively good agreement (taking into account all the approximations that have been made) with the numerical experiments. The main source of difference between theory and experiment is, most probably, the relatively big value of phase half-width: for the fourth orbit it is $\xi = 1.04$, i.e. the approximation of small phase width $\sin\xi \cong \xi$ used in our theoretical considerations is not good enough.

In this way, we have shown how the derived two-dimensional map (13) can help us to determine analytically the set of stable amplitudes of the kick-excited pendulum (3) and the stability conditions with respect to the physical parameters of the system – forcing, damping and active zone width.

It was mentioned in Section 2 that the numerical experiments with the system (3) show various stable periodic points with various (low) periods (3, 4, 5, etc.) existing around the FPs for some values of F. We have pointed out that these stable periodic

solutions in (weakly) dissipative maps correspond to elliptic points in the centers of Birkhoff islands in conservative maps. A good theoretical framework for the *multifurcations* (appearances of N-periodic Birkhoff islands near around the mother FP) in conservative maps is given by Pakarinen and Nieminen (1983). Now we want to apply the method described by them to the kick-pendulum map (13) in order to determine analytically the values of the parameter F_{3f} for which the most typical 3-periodic orbits are born. Although (13) is dissipative, its Jacobian is very close to 1 so we can expect that the results yielded by the conservative method will be relatively close to those from the numerical experiments.

Let us briefly consider the approach of Pakarinen and Nieminen. The stability of a p-cycle $\{X_1, X_2, \ldots, X_p\}$ of a two-dimensional conservative map is specified by the eigenvalues of matrix

$$(\delta x_p, \delta y_p)^{\mathrm{T}} = \hat{M}(\delta x_1, \delta y_1)^{\mathrm{T}}; \quad \hat{M} = \prod_{j=1}^{p} \hat{L}(X_j) \tag{27}$$

where $\hat{L}(X_j)$ is linearized matrix of the map around jth point X_j of the p-cycle. In the conservative case, it can be shown that the p-cycle is stable when

$$|\mathrm{Tr}\, \hat{M}| < 2 \tag{28}$$

(for proof see, for example, Lichtenberg and Lieberman, 1982, §3.3).

Suppose now that the studied map depends on some parameter μ. Suppose also that the FP is surrounded by p Birkhoff islands at a certain value of μ, hence the stability condition (28) is fulfilled. Let us now slowly vary the value of μ, so that the Birkhoff chain converges towards the "mother" FP. In the limit where the p-cycle is born, we have simply $X_1 = X_2 = \cdots = X_p = X_0$ (X_0 denotes the position of mother FP). The p-cycle becomes marginally stable, namely

$$|\mathrm{Tr}\, \hat{M}| = \left|\mathrm{Tr} \prod_{j=1}^{p} \hat{L}(X_j)\right| = |\mathrm{Tr}(\hat{L}(X_0))^p| = 2 \tag{29}$$

where $\hat{L}(X_0)$ is the linearized matrix of the original map at the mother FP. In order to determine $\mathrm{Tr}\, \hat{M}$, the following property of square 2×2 matrices

$$\mathrm{Tr}(\hat{L}_0)^p = \lambda_1^p + \lambda_2^p \tag{30}$$

is used, where λ_1 and λ_2 are eigenvalues of the matrix $\hat{L}_0$. If we write its characteristic equation in the form $\lambda^2 - T\lambda + D = 0$ (T and D denote the trace and determinant of $\hat{L}_0$, respectively) and assuming conservative map ($D = \pm 1$), we can use property (30) in order to bring the marginal stability condition down to

$$|\mathrm{Tr}\, \hat{M}| = |2(D^{1/2})^p \boldsymbol{T}_p(\tfrac{1}{2} T D^{-1/2})| = 2 \tag{31}$$

where $\boldsymbol{T}_p$ is the pth order Chebyshev polynomial of first kind (for details see Pakarinen and Nieminen, 1983). Taking advantage of the properties of Chebyshev polynomials, the last condition for $D = +1$ can be written as

$$|\mathrm{Tr}\, \hat{M}| = |2\boldsymbol{T}_p(\tfrac{1}{2} T)| = |\boldsymbol{C}_p(T)| = 2 \tag{32}$$

Here $\boldsymbol{C}_p$ denotes pth order Chebyshev polynomials of second kind. The roots of this expression, solved in order to trace of the linearized matrix T, can be immediately written as

$$T = \mathrm{Tr}\, \hat{L}(X_0) = 2\cos\left(\frac{2k\pi}{p}\right) \tag{33}$$

where k can be regarded as secondary winding number. So the last result says that there can be several marginal values of T depending on the period p of the Birkhoff chain.

Let us now apply the method described above to the studied map (13). It is not strictly conservative, but its Jacobian is very close to 1, up to the order of small dissipation. However, more crucial for the application of the method described above is the fact whether the Birkhoff attractor is born in

the very neighborhood of mother FP or the point of appearance is not so close to it. The observations from Section 2 show that, at least in case of 3-periodic orbits, they are born quite close to the mother FPs. This is not so true for the periodic points with higher periods; generally, we can speculate that the lower the period, the closer to mother FP the periodic attractor is born. So we want to apply expression (33) for 3-periodic Birkhoff chains, and we set $p=3$.

The linearization of (13) have been already found and it is given by (22); its trace has been written in the form $\mathrm{Tr}\,\hat{M} = 2 - W + BC$, where the notations of W, B and C are given by (23). Since we apply conservative analysis to a (weakly) dissipative map we can ignore the dissipation W and substituting B and C in (33), we can write

$$T = 2 + 2\pi\nu F d' \frac{\mathrm{d}K}{\mathrm{d}m}\cos\theta_l^0 = 2\cos\left(\frac{2k\pi}{3}\right) \qquad (34)$$

When $k=0$, the last equation yields exactly the saddle-node bifurcation condition for the mother point (21). When $k=1$ or 2, the cosine in the right-hand side is equal to $-1/2$, and that is the case we are interested in. Further, we can proceed in a way analogous to that used to obtain the bifurcation value F_{pd}; so after some calculations we obtain an expression for the 3-furcation parameter value F_{3f} that is very similar to those for the period doubling:

$$F_{3f}\,d' = \sqrt{[2\pi\beta m_l^0(1+m_l^0/8)]^2 + \left[\frac{12}{\pi\nu(1+9m_l^0/8)}\right]^2} \qquad (35)$$

Actually, the only difference between the expressions for F_{3f} and F_{pd} (the latter is given by (26)) is in the numerator of the second term under the radical: for period doubling we have 16 while now it is 12.

Here we can make again a test how far the theoretical prediction of the last expression is in agreement with the numerical experiments. For the fourth stable orbit which corresponds to $l=29$ and $m_l^0 = 0.378$, the last expression gives theoretical value $F_{3f}^{\mathrm{the}} = 2.31$, compared to the experimental value $F_{3f}^{\mathrm{exp}} = 2.38$, obtained in numerical simulations (see the bifurcation curve in Fig. 8). This is a very good confirmation, despite the fact that we have considered conservative version of the original dissipative map (13) in our theoretical analysis.

4. CLASS OF DISSIPATIVE TWIST MAPS

It was already shown above that the problem of kick-excited pendulum can be reduced analytically to two-dimensional map (13) under some simplifying assumptions. However, many other physical problems lead to similar maps. The most famous examples are Fermi–Ulam map modeling cosmic rays acceleration and Zaslavskii map describing the dynamics of a rotator perturbed by δ-impulses periodical in time. This section aims to view and compare the physical principles underlying these closely related problems, as well as their common features. Finally, an attempt to generalize the problems mentioned above on the basis of well-studied *dissipative twist maps* (Casdagli, 1988) will be made; moreover, this class of maps clearly shows the link between our models and the near-integrable Hamiltonian systems.

Fermi–Ulam map originates from a mechanism proposed by Fermi with the aim to explain the cosmic rays acceleration due to collisions with moving magnetic fields. There are various models of this phenomenon in the literature but the most famous is Ulam model: the accelerating particle is represented by an elastic ball bouncing between two walls, one of them fixed and the other oscillating. A simplified version of the model assumes the wall oscillations are small compared to the distance between the walls (Lichtenberg and Lieberman, 1982). This simple model preserves the most typical features of the initial problem and can be easily written for various laws of wall oscillation. In the case of sine oscillations and small linear dissipation the map has the following form (Lieberman

and Tsang, 1985):

$$\begin{aligned} u_{n+1} &= |(1-\delta)u_n + \sin\varphi_n| \\ \varphi_{n+1} &= \varphi_n + 2\pi M/u_{n+1} \pmod{2\pi} \end{aligned} \tag{36}$$

Here u is the (dimensionless) ball velocity and φ is the phase of oscillating wall, both taken at the moment of impact.

It is easy to discover several significant parallels between the Ulam model and the kick-systems map studied in previous sections. First, both maps are written in variables corresponding to oscillation energy (as $E \sim u^2$) and phase of external periodic force at the moment of injecting energy from outside. Second, the external force acts once per iteration during a time interval much less than a period of oscillation, and the system moves freely during the rest of time. Third, the period of both two systems depends on the amplitude of oscillation, hence they can be regarded as nonlinear oscillators. These important parallels prompt that we have dealt with the phenomena of the same quality.

Let us write the FPs of this map, as they are given, for example, in Lichtenberg and Lieberman (1982). The phase equation says that we have a family of stable energies: $u_m = M/m$, $m = 1, 2, \ldots$ As it has been pointed out earlier, the presence of a discrete set of FPs is a result of regarding the phase map variable by modulo. (This fact makes the maps studied here different from some others like Henon map which have not phase variables and, respectively, such families of FPs.) The values of φ_m are given by $\sin\varphi_m = \delta M/m$; the requirement $|\sin\varphi_m| \le 1$ prompts the presence of saddle-node bifurcation which produces two solutions for φ_m. It follows from the stability analysis that one of them (those with $\cos\varphi_m > 0$) is always unstable; the other ($\cos\varphi_m < 0$) is stable while $u > (\pi M/2)^{1/2}$. If we write the latter condition with respect to the parameter M, we obtain $M > \pi m^2/2$; when it turns to equality, period-doubling bifurcation takes place, followed by cascade to chaos (Lichtenberg and Lieberman, 1982). In this way, the bifurcation behavior of the FPs of (36) is qualitatively the same as those of the kick-pendulum.

Zaslavskii map originates from the problem of a mechanical oscillator under the action of periodical δ-shaped impulses written in the form

$$\begin{aligned} \dot{I} &= -\gamma(I - I_0) + \varepsilon q(I_0, \theta) f(t); \\ f(t) &= \sum_{n=-\infty}^{\infty} \delta(t - nT) \\ \dot{\theta} &= \omega(I) = \omega_0 + \frac{\alpha\omega_0}{I_0}(I - I_0) \end{aligned} \tag{37}$$

Here I and θ are action–angle variables of the autonomous oscillator, and $f(t)$ expresses the external force which has the same periodic δ-impulse shape as above. The function $q(I_0, \theta)$ is periodical in regard to the angle variable. Assuming $q(I_0, \theta) = I_0 \cos\theta$ and introducing new notations $y = (I - I_0)/I_0$, $\theta = 2\pi x$, $\Omega = \omega_0 T$ and $\Gamma = \gamma T$, we can reach the *Zaslavskii map* (Zaslavskii and Rachko, 1978):

$$\begin{aligned} y_{n+1} &= \mathrm{e}^{-\Gamma}[y_n + \varepsilon\cos(2\pi x_n)] \\ x_{n+1} &= x_n + \frac{\Omega}{2\pi} + \frac{\alpha\Omega}{2\pi}\frac{1 - \mathrm{e}^{-\Gamma}}{\Gamma} \\ &\quad \times [y_n + \varepsilon\cos(2\pi x_n)] \pmod 1 \end{aligned} \tag{38}$$

The latter system can be written in even more simple form when introducing new parameters $\omega = \Omega/2\pi$, $b = \mathrm{e}^{-\Gamma}$, $k = -(\alpha\Omega\varepsilon/(2\pi))((1 - \mathrm{e}^{-\Gamma})/\Gamma)$ and substituting $(y, x) \to (r = -ky/\varepsilon b, \theta = x + 1/2)$. That way, Zaslavskii map takes the form of DSM

$$\begin{aligned} r_{n+1} &= br_n - \frac{k}{2\pi}\sin(2\pi\theta_n) \\ \theta_{n+1} &= \theta_n + \omega + r_{n+1} \pmod 1. \end{aligned} \tag{39}$$

A very significant fact is that the approximate kick-pendulum map (14) has exactly the form of DSM. It was shown above that DSM can be obtained as a model of nonlinear oscillator under the action of periodical δ-kicks. However, we have to recall that the physical formulation of kick-systems is different: the external force acts again as short kicks but they are not strictly periodic in time due to the amplitude-dependence of the period. Actually, the impulse shape of the force is introduced in these

two systems in just opposite ways. Comparing the initial Eqs. (3) and (37), we see that in both systems the external force is represented as a product of two terms, one of them carrying the time-dependence and other the position one. In (37) the time-dependent term has impulse shape and the other is a smooth function of the position x; the situation in (3) is just opposite – the time-dependent term is a sine function while the position-dependent term is very short Π-shaped impulse. However, both the situations lead to the same discrete models, namely to DSMs.

Written as in (39) or slightly modified, DSM has been extensively studied in the last 15 years and its features are well-known. The interest is focussed on various aspects of its behavior: strange attractors and their invariant distributions (Tsang and Lieberman, 1984), transition from quasiperiodicity to chaos, destruction of invariant curves (Bohr *et al.*, 1984) and properties of the rotation interval in chaotic mode (Casdagli, 1988). The main reason for such a great interest is the simple form of map equations and clear physical meaning of the variables and parameters. The Jacobian of DSM is equal to b; therefore, the influence of dissipation on the system behavior can be studied when it changes from 1 (Hamiltonian case) to 0 (one-dimensional case). Much attention has been paid to the weakly-dissipative case where b is close to but less than 1 (Tsang and Lieberman, 1986). The two map variables can be regarded as an action–angle pair, and parameter k denotes amplitude of external nonlinear perturbation.

Let us write, following Schmidt and Wang (1985), the FPs of (39) for $\omega = 0$; one can easily see that this restriction does not change the stability conditions and qualitative behavior of the FPs but only shifts them along the angle variable θ. As it was already mentioned, the presence of angle variable leads to a family of FPs with $r_m = m$. The stability area for a given FP begins from $k_{\mathrm{sn}} = 2\pi(1-b)m$ where a pair of stable and unstable point is born, and ends at $k_{\mathrm{pd}} = 2[(\pi m(1-b))^2 + (1+b)^2]^{1/2}$ where period-doubling bifurcation takes place. It is interesting that the doubled FP undergoes a symmetry-breaking bifurcation before the next period doubling. This is because of the symmetry of the doubled solution; it has to be broken before the next period doubling. After the period-doubling cascade, the same universal boundary crisis of the strange attractor as those described in Section 1 takes place in DSM.

In addition, very large number of coexisting attractors occur for sufficiently small damping. The FP condition $r_m = m$ is fulfilled for all values of m that obey $|m| \le m_\delta = k/2\pi\delta$ (here $\delta = 1 - b$ denotes the damping); so as δ approaches zero, the interval of existence of FPs becomes very large. If we also take into account the stability analysis, we can define *stability area* for given value of k and δ as

$$\begin{aligned}\Delta m &= m_{\mathrm{sn}} - m_{\mathrm{pd}} \\ &= \begin{cases} k/2\pi\delta, & k \le 4 - 2\delta \\ k/2\pi\delta[1-[1-(4-2\delta)^2/k^2]^{1/2}], & \\ \quad k > 4 - 2\delta & \end{cases}\end{aligned} \tag{40}$$

Here m_{pd} and m_{sn} denote the limits where period-doubling and saddle-node bifurcation take place. (Clearly, we have to keep in mind that m can take only integer values.) When k is small, none of the FPs has been doubled, and m grows linearly with the force. At some value of k, the period doublings begin to destroy the FPs for small m while the saddle-node bifurcations produce them for large m; this is shown in Fig. 12. With further increase of k, the FPs are destroyed faster than they are born, and at large k the stability area decreases rapidly. Therefore, the number of simultaneously stable FPs have a maximum for some value of k.

If the solution for a fixed m is considered and the force k is varied, a *life interval* can be defined for it as

$$\Delta k = k_{\mathrm{pd}} - k_{\mathrm{sn}} = 2\pi\delta m\left\{\left[1 + \left(\frac{2-\delta}{\pi\delta m}\right)^2\right]^{1/2} - 1\right\} \tag{41}$$

where k_{pd} and k_{sn} are the parameter values for period doubling and saddle-node bifurcation,

respectively. It is clear from this expression that the life interval decreases when increasing the damping; actually, we can speculate that the same is right for periodic points with arbitrary period but not only for the FPs.

It can be easily seen that all the maps examined throughout this paper – namely, Fermi–Ulam map (36), DSM (39) and the kicked pendulum map (13) – can be written in a general form:

$$\begin{aligned} J_{n+1} &= (1-\delta)J_n + \varepsilon f(\theta_n) \\ \theta_{n+1} &= \theta_n + 2\pi\alpha(J_{n+1}) \pmod{2\pi} \end{aligned} \tag{42}$$

This notation clearly reveals the physical basis of the systems. The periodic function of the phase variable $f(\theta)$ expresses the injection of energy due to external periodic force; the parameter ε is introduced as an amplitude of the perturbing force. Here the small damping is considered as linear: $\delta = \text{const.}$, but this parameter can depend weakly on the energy variable, as it happens in the kick-pendulum map. The function $\alpha(J)$ expresses the amplitude-dependence of the period of oscillations

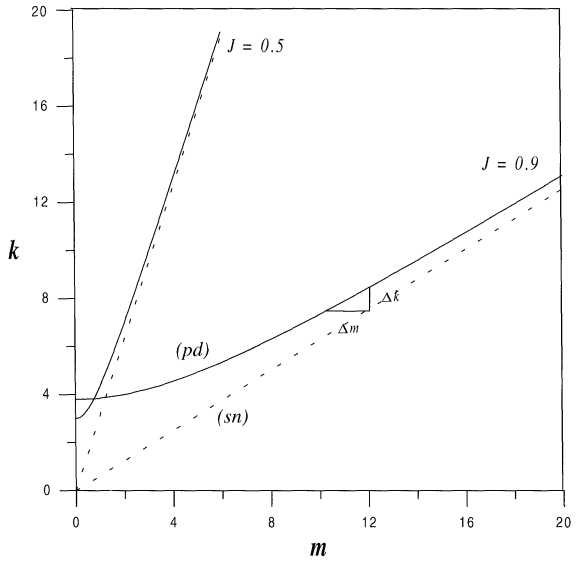

FIGURE 12 Graphical representation of the saddle-node and period-doubling bifurcation parameters for all family of FPs in DSM for two different values of the Jacobian.

and it is responsible for the appearance of a discrete set of FPs with different values of the energy. Moreover, (42) is not accidentally written in this form: similar discrete maps naturally arise from the analysis of near-integrable Hamiltonian systems with two degrees of freedom. Since the kick-systems studied here can be also regarded as Hamiltonian systems with small dissipative perturbation, let us briefly outline the correspondence between cannonical systems and two-dimensional maps of this special kind.

If an autonomous Hamiltonian system is integrable, cannonical variables action–angle (J_i, θ_i) can be introduced so that the full energy would not depend on the angle variables; the action variables J_i are integrals of motion. In case of two degrees of freedom the trajectory is confined to a two-dimensional torus. If we introduce Poincaré surface that intersects the torus at fixed value of the variable $\theta_i = \text{const.}$, the map for the rest of the pairs of action–angle variables takes the form of so-called *twist map*: $(J_{n+1} = J_n; \quad \theta_{n+1} = \theta_n + 2\pi\alpha(J_{n+1}))$ (Lichtenberg and Lieberman, 1982). If a small perturbation is added to the integrable system, the twist map changes to its perturbed version

$$\begin{aligned} J_{n+1} &= J_n + \varepsilon f(J_{n+1}, \theta_n) \\ \theta_{n+1} &= \theta_n + 2\pi\alpha(J_{n+1}) + \varepsilon g(J_{n+1}, \theta_n) \end{aligned} \tag{43}$$

where f and g are periodic functions of θ.

It appears that in many interesting cases f does not depend on J and $g = 0$; such a map is known as a *radial twist map*. Adding a linear dissipation term, we obtain exactly the map (42) which will be referred further as a *dissipative twist map*.

The idea of twist maps can be expressed in other way, without considering perturbed Hamiltonian systems and even without assuming any particular form similar to (42). For example, Casdagli (1988), following some works of Birkhoff, defines the twist maps as diffeomorphisms acting on the unit cylinder and having some special properties. The most interesting among them is so-called *twist hypothesis*; it says that the image of any vertical straight line under the map is a curve sloping strictly to the

right. If the Jacobian is everywhere less than some $\lambda < 1$, and if in addition the motion is limited along the cylinder axis variable (in order to guarantee existence of attracting sets), we have dissipative twist maps.

It is interesting that in the light of the latter definition the kick-pendulum map (13) is not exactly a twist map. Indeed, it can be shown that it violates the twist hypothesis. First, we must remark that for a map in the form (42) this hypothesis requires the function $\alpha(J)$ expressing the amplitude-dependence of the period to be monotonous. However, we have dealt with a pendulum, and its period of free motion is equal to $4K(m)$ only for $m < 1$ (here $K(m)$ is the complete elliptic integral of first kind), i.e. when no rotation around the hanging point takes place. When $m > 1$ (rotation mode), the period is $(1/m)K(1/m)$, while for $m = 1$ it goes to infinity. If we consider motions in pure oscillation ($m < 1$) or pure rotation ($m > 1$) mode, the twist hypothesis is fulfilled. However, the presence of peculiar point $m = 1$ changes the qualitative character of motion in its vicinity. This case corresponds to a motion near the separatrices of hyperbolic FP corresponding to the top (unstable) equilibrium point of the pendulum. In this case, homoclinic intersections between the separatrices become possible at some parameter values, and chaotic oscillations can take place. (Strictly speaking, the intersection of separatrices is neither necessary nor sufficient condition for appearance of strange attractor, but in many cases it precedes the chaotization of the system.) However, we do not consider the separatrix chaos in this paper, and for that reason we have restricted our study of the kick-pendulum only to the interval $m < 1$.

If we recall the latter hypothesis we see that it plays some kind of role in determining the FPs of (42). The phase equation yields $\alpha(J_m) = m$, where m is an integer. The set of fixed values of the action J_m can be obtained from this condition – but only if a unique inverse function $J = \alpha^{-1}(m)$ exists in the whole action interval considered. This requires $\alpha(J)$ being monotonous or, in other words, the twist hypothesis being fulfilled.

5. THE GENERAL KICK-MODEL AS A TWIST MAP

It has been shown already that the problem of kicked pendulum – a particular case of kick-system – can be reduced to a discrete twist map. The analysis was based on the energy balance and amplitude-dependence of the period, and the assumption of narrow active zone has been essentially used. In this section we want to apply this technology to the problem of kick-excitation in the general form proposed as (1) and (2). Recall that the general kick-system has been written as

$$\begin{aligned} &\ddot{x} + 2\beta\dot{x} + f(x) = \varepsilon(x) \cdot \Pi(\nu t); \\ &\varepsilon(x) = 0, \ |x| > d' \quad (d' \ll x_{\max}) \end{aligned} \tag{44}$$

So the goal is to *derive discrete map describing in general the wide class of kick-excited systems*, if the nonlinear returning force $f(x)$, feeding function $\varepsilon(x)$ and shape of the periodic force $\Pi(\nu t)$ are not fixed but vary.

Recall the way of deriving the map (13) for the kicked pendulum. The map variables express the oscillation energy and the external phase, respectively. Now we have to make some assumptions concerning the nonlinear returning force $f(x)$ and periodic function $\Pi(\nu t)$ which will be used further. We shall assume $f(x) = \partial U/\partial x$ in (1) corresponds to a potential $U(x)$ that has a unique minimum at zero: $U(0) = 0$ and is symmetric with regard to it. In addition, we shall assume symmetric feeding function $\varepsilon(x)$ and $\Pi(\nu t)$ changing its sign for a half-period: $\Pi(\nu t + \pi) = -\Pi(\nu t)$. These conditions are introduced in order to assure invariance of (44) under transformation $(x, \dot{x}, \varphi) \to (-x, -\dot{x}, \varphi + \pi)$. We will use such a symmetry of the kick-system in order to make the map iterations standing for a half-period instead of a full period of oscillation, as it has been done in previous sections. Under these assumptions the evolution of the phase variable is given by

$$\theta_{n+1} - \theta_n = \nu \frac{T(E)}{2} + \pi \tag{45}$$

where $T(E)$ is the period of oscillations expressed as a function of energy, and additional shift with π is introduced due to the symmetry of (44) assumed above. As the active zone is accepted to be sufficiently narrow, $T(E)$ is simply the period of free oscillation, and it can be expressed as a function of energy:

$$T(E) = 2\sqrt{2}\int_0^{x_{\max}} (E - U(x))^{-1/2}\,\mathrm{d}x \qquad (46)$$

where $x_{\max}$ denotes the turning point of oscillations. We can also choose the energy variable iterations in such a way that the phase evolution given by (45) depends on the $(n+1)$th value of E but not on the nth one. This way, the phase equation can be written as

$$\theta_{n+1} = \theta_n + 2\pi\alpha(E_{n+1}); \quad \alpha(E) = \nu\frac{T(E)}{4\pi} + \frac{1}{2} \qquad (47)$$

Let us now consider the energy balance. The energy received in the active zone can be found by integrating right-hand side of (44) over the zone width and assuming small phase half-width:

$$\Delta E_{\text{in}} = \int_{-d}^{d} \Pi(\nu t(x))\varepsilon(x)\,\mathrm{d}x \cong \Pi(\theta)\int_{-d}^{d}\varepsilon(x)\,\mathrm{d}x \qquad (48)$$

We can speculate that the integral in the right-hand side is proportional to the forcing amplitude $F = \max(\varepsilon(x))$, as well as to the zone width d'. Hence, the energy received can be written as $\Delta E_{\text{in}} = \gamma F d' \Pi(\theta)$, where the factor γ depends only on the profile of $\varepsilon(x)$. If, for example, $\varepsilon(x)$ is Π-shaped, then simply $\gamma = 2$.

Now, we must estimate the energy dissipation. Generally, it is specific for every particular oscillating force, i.e. for every potential well. However, we consider the small damping case $0 < \beta \ll 1$, and we can assume small *linear* dissipation $\Delta E_{\text{out}} = \delta E$ with $\delta \approx \beta T$. (Here the period T generally depends on E but we regard it as nearly constant in order to write out the dissipation in linear form.) Now we can write the energy balance equation, and joining it to the phase equation (47) we arrive at a map identical with the dissipative twist map (42):

$$\begin{aligned} E_{n+1} &= (1-\delta)E_n + \varepsilon\Pi(\theta_n) \\ \theta_{n+1} &= \theta_n + 2\pi\alpha(E_{n+1}) \pmod{2\pi} \end{aligned} \qquad (49)$$

with following notations introduced:

$$\varepsilon = \gamma F d'; \quad \alpha(E) = \nu\frac{T(E)}{4\pi} + \frac{1}{2} \qquad (50)$$

So it becomes clear that *dissipative twist map* (49) *models the general kick-system* (44) *with symmetric potential well, small dissipation and thin active zone.*

This is a very important result. It puts the class of kick-excited systems in correspondence to the well-studied class of dissipative twist maps. It also clears the fact that kick-systems inherit their common features from the twist maps. So we can assert that it is convenient to consider the system (49) as a *general kick-model* which stands for a variety of physical systems and especially of those forced in impulse way, i.e. the external force acts only for short time impulses.

6. CONCLUSION

As a conclusion, we will present a brief list of the common features of the kick-excited systems following the twist map model:

- a set of stable FPs exist, with energies determined by $\alpha(E_m) = m$. Their existence is a consequence of regarding the phase variable only by modulo;
- the stationary values of energy do not depend on the external force F because they are determined only by the function $\alpha(E)$ depending only on the external frequency and the shape of the potential well;
- if a small damping δ is fixed, the FPs are born after saddle-node bifurcation when varying F (or ε, which is the same). That follows from

the condition of stationary phase $\delta E_m = \varepsilon\Pi(\theta_m)$; the periodic function $\Pi(\theta)$ is bounded so that the requirement for existence of FPs imposes a lower boundary for F as $\varepsilon \geq \delta E_m/\max(\Pi(\theta))$;

- when F is further increased the FPs become unstable via period-doubling bifurcation. This can be seen from the linearized matrix of (49) which is

$$\hat{M} = \begin{pmatrix} 1-\delta & \varepsilon\Pi'(\theta^0) \\ 2\pi\alpha'(E^0)(1-\delta) & 1+2\pi\alpha'(E^0)\varepsilon\Pi'(\theta^0) \end{pmatrix} \tag{51}$$

Note that $\mathrm{Tr}\,\hat{M} = 2-\delta+2\pi\alpha'(E^0)\varepsilon\Pi'(\theta^0)$ and $\det\hat{M} = 1-\delta$. The study of linear stability implies the inequality $|\mathrm{Tr}\,\hat{M}| < 1+\det\hat{M} = 2-\delta$ which yields

$$0 > \pi\alpha'(E^0)\varepsilon\Pi'(\theta^0) > -(2-\delta) \tag{52}$$

Here the left inequality gives the saddle-node bifurcation point and the right one the period-doubling point;

- period-doubling cascade leading to strange attractors occur after losing stability; later the attractor is destroyed via universal boundary crisis. The smaller the damping, the shorter is the chaotic interval of parameter values.

It is also useful to outline the influence of physical parameters of the initial kick-system (44) upon the resulting kick-model (49):

- the damping δ reflects on the number of coexisting attractors for given F: smaller the damping, greater the number of attractors. This effect has been fully described above for the DSM; in the general kick-model it is qualitatively similar but the number of coexisting points and its life interval vary. It has to be mentioned that small damping leads to slow convergence to the stable modes and to long chaotic transients;
- the zone width d' has to be chosen sufficiently small in order to obey the small phase width condition $\xi = \nu d'/\bar{v}$. Clearly, ξ also depends on the frequency ν and on the velocity in the zone, hence on the energy. It can happen that the small phase width condition is violated for lower energies but holds for higher ones;
- the external force amplitude F, together with zone width d' and geometric factor γ, constitutes the small parameter ε. This parameter introduces nonlinear perturbation in the system and therefore F has the meaning of an external nonlinearity which destroys the stable attractors;
- the external frequency ν, together with the amplitude-dependence of the period, determines, in accordance with (50), the twisting rate function $\alpha(E)$; the latter, in its turn, specifies the set of stationary energy values as $\alpha(E_m) = m$. Since $\alpha(E) \sim \nu$ (see (50)), higher frequencies lead to denser sets of fixed energies. However, another effect exists that is caused by the fact that ν, together with $\alpha'(E)$, stays in expression (52) specifying the stability of the FPs. These speculations come to tell us that some optimal value of ν with highest number of simultaneously stable attractors must exist. However, we have to know the exact form of period dependence $T(E)$ in order to estimate this effect more precisely.

Finally, let us briefly discuss the influence of the functions varied in general kick-system (44) over the system dynamics:

- the nonlinear returning force $f(x)$ is related to the potential as $f(x) = \partial U/\partial x$. The shape of the potential well governs, in accordance to (46), the amplitude-dependence of the period, hence the twisting rate $\alpha(E)$ and the set of stationary energies. It is interesting to examine numerically the behavior of a system with different potential well from those of the pendulum. The bifurcation diagram for the kicked Duffing oscillator with single potential well is presented in Fig. 13. In this case $U(x) = x^2/2 + x^4/4$; contrary to the pendulum, in this case the period decreases when increasing energy. Besides that, the function $T(E)$ has no peculiarities like approaching infinity at some finite value of E due to motion near a separatrix because the potential has only

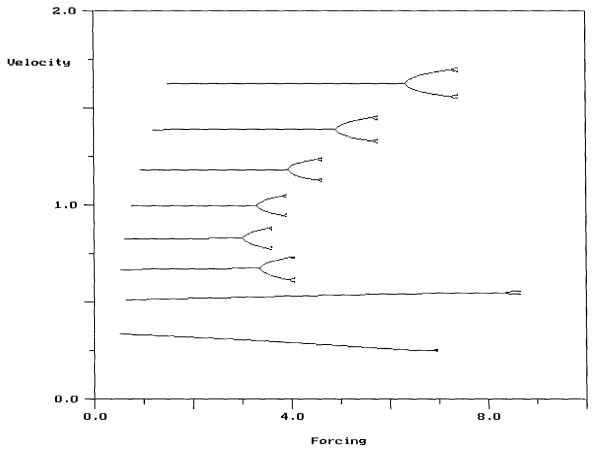

FIGURE 13 A multiple bifurcation diagram for kicked Duffing oscillator with single potential well.

a single minimum and any other hyperbolic points. It is seen in Fig. 13 how, contrary to the pendulum case examined in Section 1, the FPs are more densely distributed for lower energies and more sparsely for higher ones; in addition, the FPs with lower energies lose stability earlier. It can be easily shown that all these differences are due to the negative first derivative and positive second derivative of $T(E)$ which reflect on the stationarity condition $\alpha(E_m) = m$ and stability condition (52), respectively;

- the feeding function $\varepsilon(x)$ reflects only on the value of factor γ which depends on its shape. This factor takes the maximum value $\gamma = 2$ for Π-shaped feeding function;
- the time-periodic law $\Pi(\theta)$ determines, by virtue of (49), the fixed values of the phase variable. If we assume that $\Pi(\theta)$ is continuous in $[0, 2\pi]$ and has only one minimum and one maximum in this interval, according to (49) we shall have either two or no fixed values of θ. (The former case corresponds to pair of stable and unstable FPs.) However, if $\Pi(\theta)$ has more complex shape, the stationarity condition can produce neither two nor zero solutions but some other number of them. This effect may cause the appearance of several stable points for a definite stationary energy E_m; recall that E_m is determined by $\alpha(E_m) = m$ and does not depend in any way on the phase variable value.

References

Blackburn, J.A., Smith, H.J.T. and Gronbech-Jensen, N. (1992). Stability and Hopf bifurcation in an inverted pendulum. *Am. J. Physics*, **60**(10), 422–426.

Bohr, T., Bak, P. and Jensen, M.H. (1984). Transition to chaos by interaction of resonances in dissipative systems. II. Josephson junctions, charge-density waves, and standard maps. *Phys. Rev. A*, **30**, 1970.

Bruk, G. (1990). *Cyclic Accelerators of Charged Particles.* Atomizdat, Moscow, pp. 33–73.

Butenin, N.V., Neymark, Y.I. and Fufaev, N.A. (1987). *Introduction to Theory of Nonlinear Oscillations.* Nauka Publisher, Moscow, pp. 81–112.

Casdagli, M. (1988). Rotational chaos in dissipative systems. *Physica D*, **29**, 365.

Cecchi, G.A., Gonzales, D.L., Magnasco, M.O., Mindlin, G.B., Piro, O. and Santillan, A.J. (1993). Periodically kicked hard oscillators. *Chaos*, **3**(1), 51–62.

Chen, C., Gyorgyi, G. and Schmidt, G. (1986). Universal transition between Hamiltonian and dissipative chaos. *Phys. Rev. A*, **34**, 2568.

Chua, L.O. (1987). *Linear and Nonlinear Circuits.* University of California, Berkeley, pp. 17–171.

Damgov, V.N., Douboshinsky, D.B. and Douboshinsky, Y.B. (1986). Excitation of stationary oscillating motion by action with periodic force, nonlinear to coordinates. *Comptes Rendus de l'Academie Bulgare des Sciences*, **39**(10), 63–66.

Damgov, V.N. and Grinberg, G.S. (1991). Method of continuous oscillation excitation in linear dissipative systems with adaptive pumping. *Comptes Rendus de l'Academie Bulgare des Sciences*, **44**(9), 33–36.

Damgov, V.N. and Douboshinsky, D.B. (1992). The wave nature and dynamical quantization of the Solar System. *Earth, Moon and Planets*, **56**, 233–242.

Grebogi, C., Ott, E. and Yorke, J.A. (1983). Crises, sudden changes of chaotic attractors and transients to chaos. *Physica D*, **7**, 181.

Gumowsky, I. (1989). *Oscillatory Evolutional Processes. Quantitative Analysis Arising from Applied Sciences.* Manchester University Press, pp. 49–91.

Hagedorn, P. (1988). *Nonlinear Oscillations.* Clarendon Press, Oxford, pp. 35–77.

Hastings, S.P. and McLeod, J.B. (1993). Chaotic motion of a pendulum with oscillatory forcing. *American Math. Monthly*, **100**(6), 563–572.

Heng, H., Doerner, R., Hüblinger, R. and Martienssen, W. (1994). Approaching nonlinear dynamics by studying the motion of a pendulum. I. Observing trajectories in state space. *Int. J. Bifurcation Chaos*, **4**(4), 751.

Holmes, P.J. (1982). The dynamics of repeated impacts with a sinusoidally vibrating table. *J. Sounds Vibrations*, **84**(2), 173–189.

Isomäki, H.M., von Boehm, J. and Raty, R. (1985). Devil's attractors and chaos of a driven impact oscillator. *Phys. Lett. A*, **107**(8), 343–346.

Isomäki, H.M. (1990). Fractal properties of the bouncing-ball dynamics. In: *Nonlinear Dynamics in Engineering Systems* (W. Schiehlen, Ed.), Springer, Berlin, pp. 61–96.

Kanavetz, V., Mozgovoy, Y. and Slepkov, A. (1991). *Radiation of Powerful Electron Flows in Resonance Delay Systems*. MGU Publisher, Moscow, pp. 39–121.

Kapitaniak, T. (1991). *Chaotic Oscillations in Mechanical Systems*. Manchester University Press, pp. 19–93.

Landa, P.S. and Douboshinsky, Y.B. (1989). Self-oscillating systems with HF power source. *UFN* (*Soviet Physics-Uspehi*), **158**(4), 729–742.

Liao, S.J. (1992). A second-order approximate analytical solution of a simple pendulum by the process analysis method. *J. Applied Mechanics*, *Transactions of the ASME*, **59**, 970–975.

Lichtenberg, A.J. and Lieberman, M.A. (1982). *Regular and Stochastic Motion*. Springer-Verlag, New York.

Lieberman, M.A. and Tsang, K.Y. (1985). Transient chaos in dissipatively perturbed near-integrable Hamiltonian systems, *Phys. Rev. Lett.*, **55**, 908.

Mawhin, J. (1993). Nonlinear oscillations: one hundred years after Liapunov and Poincaré. *Zeitschrift für Angewantte Mathematik und Mechanik* (*ZAMM*), **73**(4–5), T54–T62.

McDonald, S.W., Grebogi, C., Ott, E. and Yorke, J.A. (1985). Fractal basin boundaries. *Physica D*, **17**, 125.

Migulin, V.V., Medvedev, V.Y., Mustel, E.R. and Parigin, V.N. (1983). *Basic Theory of Oscillations*, World Scientific Notes in Physics, pp. 991–176.

Minorsky, N. (1962). *Nonlinear Oscillations*. D. van Nostrand Inc., N.Y., pp. 495–501.

Miroshin, R. and Halidov, I. (1991). *Theory of Local Interactions*. Sankt-Petersburg State University Publisher, Sankt-Petersburg, pp. 12–192.

Morozov, A.D. (1990). On resonance, pendulum equations, limit cycles and chaos. In: *Research Reports in Physics*, *Nonlinear Waves* (A.V. Gaponov-Grekhov *et al.*, Eds.), Springer-Verlag, Berlin, pp. 276–282.

Pakarinen, P. and Nieminen, R.M. (1983). Period-multiplying bifurcations and multifurcations in conservative mappings. *J. Phys.*, **16**, 2105.

Schmidt, G. and Wang, B.W. (1985). Dissipative standard maps. *Phys. Rev. A*, **32**, 2994.

Schuster, H.G. (1984). *Deterministic Chaos*. Physik-Verlag, Weinheim.

Sikri, A.K. and Narchal, M.L. (1993). Floquet states of a periodically kicked particle. *Pramana-Journal of Physics*, **40**(4), 267–272.

Soliman, M.S. and Thompson, J.M.T. (1992). The effect of damping on the steady state and basin bifurcation patterns of a nonlinear mechanical oscillator. *Int. J. Bifurcation Chaos*, **2**(1), 81–91.

Strijak, T.G. (1981). *Method for Investigation of Dynamical Systems of Pendulum Type*. Nauka Publisher, Alma Ata, pp. 18–188.

Troesch, A.W., Karr, D.G. and Beier, K.-P. (1992). Global contact dynamics of an ice–structure interaction model. *Int. J. Bifurcation Chaos*, **2**(3), 607–620.

Tsang, K.Y. and Lieberman, M.A. (1984). Analytical calculation of invariant distributions on strange attractors. *Physica D*, **11**, 147.

Tsang, K.Y. and Lieberman, M.A. (1986). Transient chaotic distributions in dissipative systems. *Physica D*, **21**, 401.

Tung, P. (1992). Dynamics of a nonharmonically forced impact oscillator. *JSME Int. J.*, Series III, **35**(3), 378–386.

Vaynshtein, L.A. and Vakman, D.E. (1983). *Frequency Division in the Theory of Oscillations and Waves*. Nauka Publisher, Moscow, pp. 79–93.

Yip, S.C. and Dimaggio, F. (1993). Routes to chaos of a pendulum with vertically rotating pivot. *Computers and Structures*, **46**(4), 725–740.

Zaslavskii, G.M. and Rachko, Kh.R.Ya. (1978). Singularities of the transition to a turbulent motion. *Sov. Phys. JETP*, **49**, 1039.